CHAPTER 15

Efficient earthquake intensity measures for probabilistic seismic demand models of skewed RC bridges

Van-Tien Phan, Xuan-Hung Vu, Tien-Hong Nguyen, Trong-Cuong Vo and Duy-Duan Nguyen
Department of Civil Engineering, Vinh University, Vinh, Nghe An, Vietnam

1. Introduction

The worldwide seismic design codes and seismic structural analysis procedures commonly use the peak ground acceleration (PGA) or spectral acceleration (S_a) as the seismic intensity measures (IMs). Also, these IMs are widely employed for the seismic fragility assessment of infrastructures (Lee & Nguyen, 2018; Nguyen & Lee, 2018; Tran et al., 2021). However, many studies demonstrated that PGA or S_a may not always be the best options for the seismic design and fragility analyses of structures (Cao & Ronagh, 2014; Elenas & Meskouris, 2001; Ghayoomi & Dashti, 2015; Massumi & Gholami, 2016; Nguyen, Thusa et al., 2020; Nguyen, Azad et al., 2020). Numerous studies were conducted to evaluate the interrelation between seismic IMs and seismic responses of buildings (Cao & Ronagh, 2014; Elenas, 2000; Elenas & Meskouris, 2001; Kostinakis et al., 2015; Massumi & Gholami, 2016; Pejovic et al., 2017), tunnels (Chen & Wei, 2013; Nguyen et al., 2019), on-ground liquid storage tanks (Phan & Paolacci, 2016), pipelines (Shakib & Jahangiri, 2016), and nuclear power plant structures (Nguyen, Thusa et al., 2020; Nguyen, Azad et al., 2020), and chimneys (Qiu et al., 2020).

The correlation between seismic IMs and damage of bridges was carried out intensively. Padgett et al. (2008) evaluated optimal IMs for generating probabilistic seismic demand models for bridge portfolios through a multi-span simply supported steel girder bridge. Considering synthetic and recorded ground motions, they concluded that PGA and $S_a(T_1)$ are the most optimal for the synthetic motions, while cumulative absolute velocity (CAV) is the

Multi-Hazard Vulnerability and Resilience Building
ISBN 978-0-323-95682-6
https://doi.org/10.1016/B978-0-323-95682-6.00004-8

most reliable for using recorded motions. Zhang et al. (2015) investigated the correlation between seismic IMs of far-fault motions and the damage of a cable-stayed bridge with a single pylon in China. The best correlated IMs exhibited were velocity spectral intensity (VSI), S_a(T1), and HI. Jahangiri et al. (2018) pointed out that root mean square of acceleration (A_{rms}) is the optimal IM for seismic response assessment of plain concrete arch bridges. In the study of Zelaschi et al. (2019), considering a set of Italian RC bridges and using 30 ground motions scaled to the conditional spectrum, they pointed out that the Fajfar index (I_v), PGV, and S_a are the optimal IMs. Avsar and Özdemir (2013) highlighted that accelerated-related IMs are not well correlated with the response of seismic-isolated bridges. Additionally, the period-dependent IMs, such as VSI, HI, modified acceleration spectrum intensity (MASI), and S_a are strongly correlated with the maximum isolator displacement of seismic-isolated bridges for ordinary records, whereas PGV and modified velocity spectrum intensity (MVSI) are strongly correlated IMs for pulse like ground motions. Recently, Wei et al. (2020) evaluated optimal earthquake IMs for fragility analysis of a multipylon cable-stayed bridge with super high piers.

Numerous studies on seismic performances of skewed bridges were implemented (Abdel-Mohti & Pekcan, 2008, 2013; Bayat & Daneshjoo, 2015; Chen & Chen, 2016; Kawashima & Tirasit, 2008; Kun et al., 2018; Wang et al., 2020; Wilson et al., 2014, 2015; Zakeri et al., 2015). However, studies on the correlation between earthquake IMs and seismic responses of skewed bridges have been very limited so far. The purpose of this study is to develop probabilistic seismic demand models of 20 earthquake IMs and seismic responses of a skewed RC bridge. For that, a set of 90 ground motion records, which contain a wide range of amplitudes, magnitudes, epicentral distances, significant durations, and predominant periods, are used to perform nonlinear time-history analyses. Based on the probabilistic seismic demand model, the efficient IMs for seismic responses of the bridge are identified Fig. 15.1.

2. Skewed bridge configuration

The studied bridge includes 11 spans with the RC slab and 10 R C circular triple-column bents. The length of all spans is 14.5 m, and the total length of the bridge is 159.5 m. The height of columns is varied from 4.0 to 6.0 m.

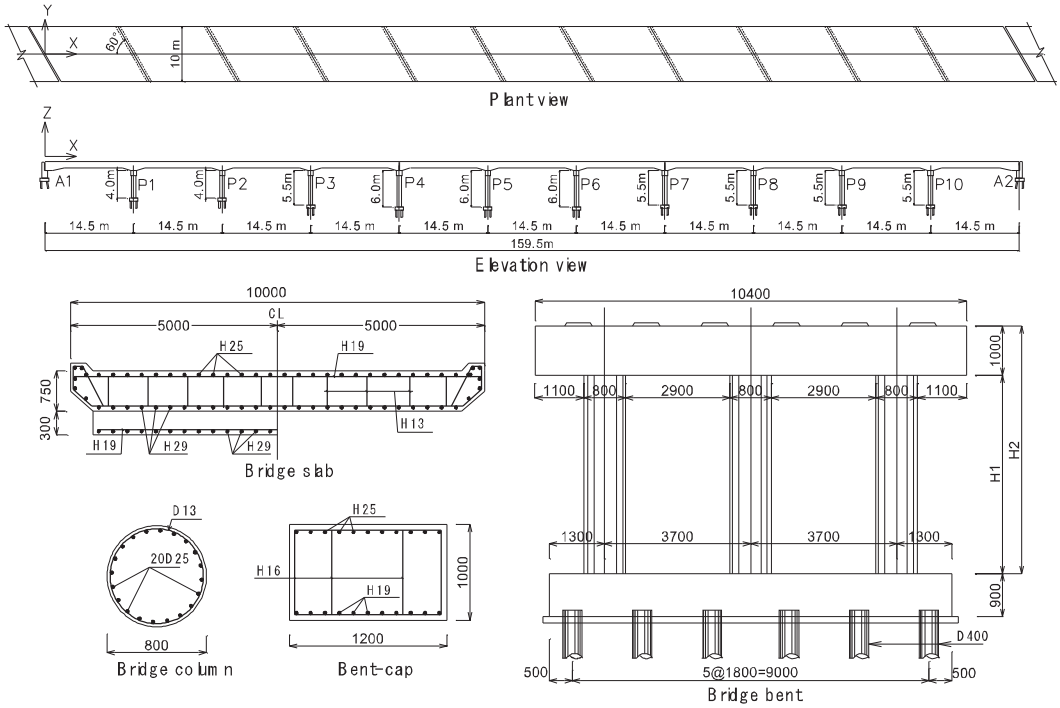

Figure 15.1 Configurations of the skewed bridge.

The bridge is skewed with an angle of 60°, as shown in Fig. 15.2. The detailed dimensions of the girders, pier columns, and the bent cap are also shown in Fig. 15.2. For the foundation of bridge bents, 12 bored piles ($D = 0.4$ m) arranged in a double-row are connected with the pile-cap the dimensions of which are height, width, and length are 0.9, 2.5, and 10 m, respectively. The length of piles is reduced from 22 m (at the bent P1) to 10 m (at the bent P10). The piles are mostly embedded into sand, gravel-sand, amber gravel, weathered rock, and soft rock layers.

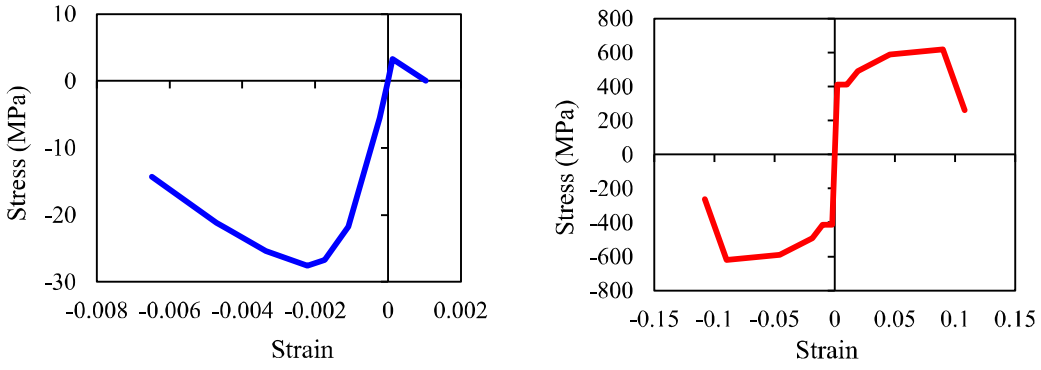

Figure 15.2 Material models for concrete and reinforcement.

3. Numerical modeling

The numerical model of the bridge is developed using SAP2000, the finite element analysis program (CSI, 2015). The bridge slab is modeled using a series of elastic shell elements. Meanwhile, the bridge piers are modeled as nonlinear beam–column elements. For that, the model proposed by Mander et al. (1988) is adopted for nonlinear concrete material, while the reinforcement material model presented in Park and Pauley (1975) is applied for reinforcing bars. Fig. 15.2 shows the stress–strain curves of the concrete and steel models. The moment–curvature relationship of bridge piers is illustrated in Fig. 15.3. Moreover, to consider soil–structure interaction, the piles are also modeled in terms of elastic beam elements, in which the linear soil springs are attached to the pile element nodes. It should be noted that the foundations of the selected bridge are mostly embedded in the dense sand and weathered-rock layers. The 3D finite element modeling of the bridge in SAP2000 and modal analysis results are shown in Figs. 15.4 and 15.5, respectively.

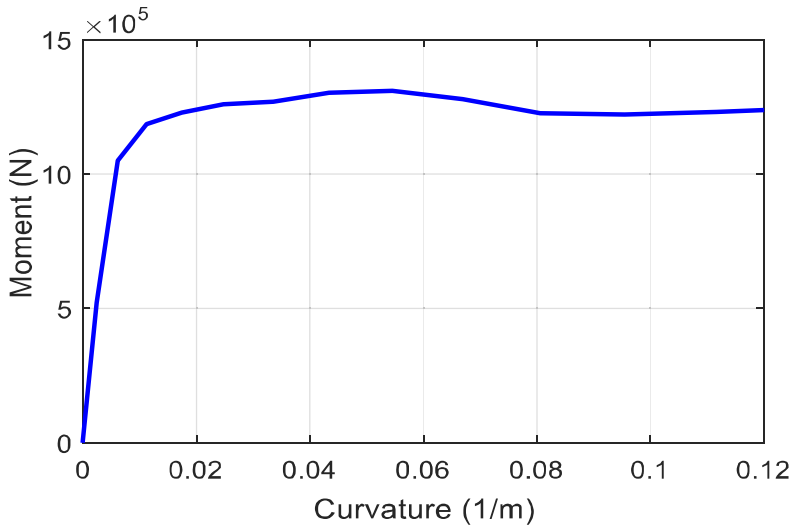

Figure 15.3 Moment-curvature relationship of bridge piers.

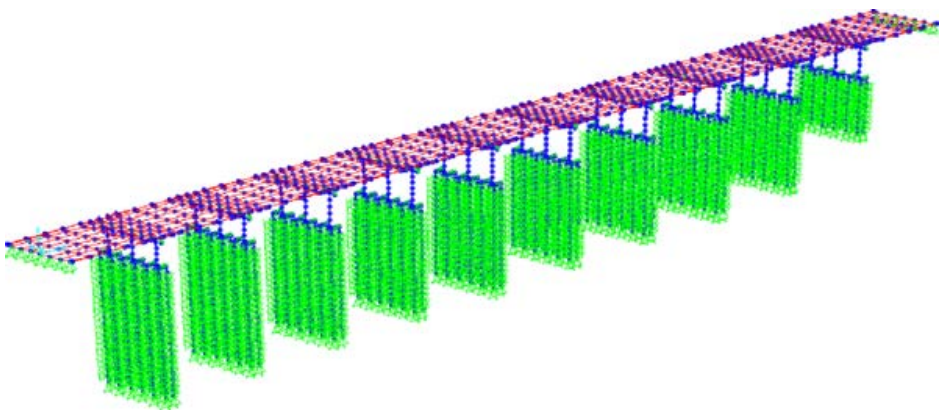

Figure 15.4 3D finite element model of the skewed bridge.

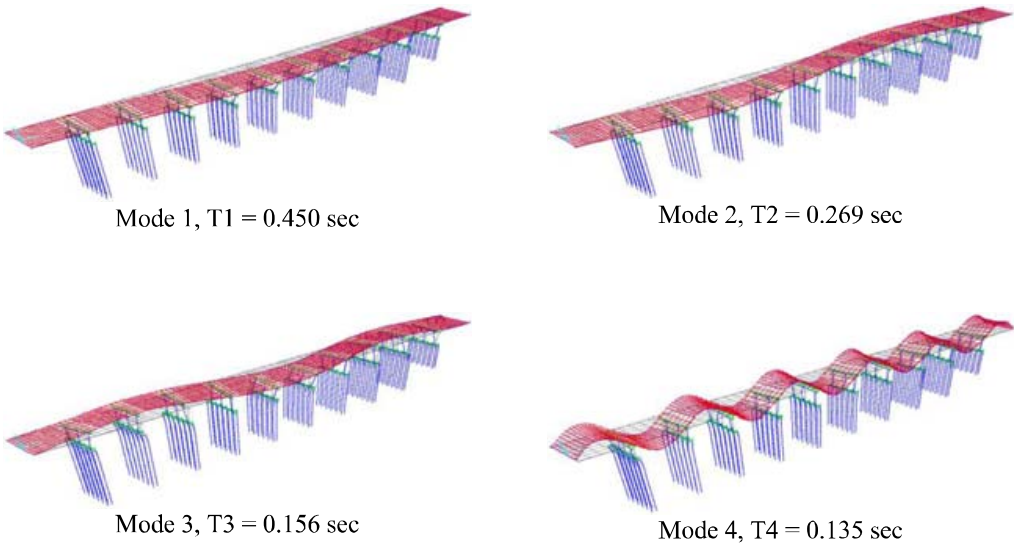

Figure 15.5 Eigenvalue analysis results.

4. Earthquake intensity measure and ground motions

4.1 Intensity measures

Earthquake intensity measures (IMs) are fundamental for describing the important characteristics of ground motion in a quantitative manner. Many IMs have been proposed to characterize the amplitude, frequency content, and duration of motions (Kramer, 1996). To obtain the seismic IMs, a direct evaluation from earthquake accelerograms and a calculation by the software can be implemented. This study accounts for 20 common ground motion IMs and these parameters are calculated for every motion record using the SeismoSignal program (SeismoSignal, 2017). The used IMs and their definitions are presented in Table 15.1.

4.2 Ground motions

In this study, 90 ground motion records provided by the PEER center database (PEER, 2019) are selected for time-history analyses. A wide range of earthquake amplitudes, magnitudes, epicentral distances, significant durations, predominant periods are considered in used ground motions. The ranges of those parameters are as follows.

- $0.093g \leq PGA \leq 1.585g$
- $0.25 \leq PGA/PGV \leq 3.294$

Table 15.1 Earthquake intensity measures.

No.	Earthquake parameter	Definition	Unit	Reference
1	Peak ground acceleration	$\mathrm{PGA} = \max \lvert a(t) \rvert$	g	—
2	Peak ground velocity	$\mathrm{PGV} = \max \lvert v(t) \rvert$	m/s	—
3	Peak ground displacement	$\mathrm{PGD} = \max \lvert d(t) \rvert$	m	—
4	Root mean square of acceleration	$A_{rms} = \sqrt{\frac{1}{t_{tot}} \int_0^{t_{tot}} a(t)^2 dt}$	g	Dobry et al. (1978)
5	Root mean square of velocity	$V_{rms} = \sqrt{\frac{1}{t_{tot}} \int_0^{t_{tot}} v(t)^2 dt}$	m/s	Kramer (1996)
6	Root mean square of displacement	$D_{rms} = \sqrt{\frac{1}{t_{tot}} \int_0^{t_{tot}} d(t)^2 dt}$	m	Kramer (1996)
7	Arias intensity	$I_a = \frac{\pi}{2g} \int_0^{t_{tot}} a(t)^2 dt$	m/s	Arias (1970)
8	Characteristic intensity	$I_c = (A_{rms})^{3/2} \sqrt{t_{tot}}$	$m^{1.5}/s^{2.5}$	Park et al. (1985)
9	Specific energy density	$\mathrm{SED} = \int_0^{t_{tot}} v(t)^2 dt$	m^2/s	—
10	Cumulative absolute velocity	$\mathrm{CAV} = \int_0^{t_{tot}} \lvert a(t) \rvert dt$	m/s	Benjamin (1988)
11	Acceleration spectrum intensity	$\mathrm{ASI} = \int_{0.1}^{0.5} S_a(\xi = 0.05,\ T) dT$	g*s	Thun et al. (1988)
12	Velocity spectrum intensity	$\mathrm{VSI} = \int_{0.1}^{2.5} S_v(\xi = 0.05,\ T) dT$	m	Thun et al. (1988)
13	Housner spectrum intensity	$\mathrm{HI} = \int_{0.1}^{2.5} PS_v(\xi = 0.05,\ T) dT$	m	Housner (1952)
14	Sustained maximum acceleration	SMA = the 3rd of PGA	g	Nuttli (1979)
15	Sustained maximum velocity	SMV = the 3rd of PGV	m/s	Nuttli (1979)
16	Effective peak acceleration	$\mathrm{EPA} = \frac{mean\left(S_a^{0.1-0.5}(\xi=0.05)\right)}{2.5}$	g	Benjamin (1988)

Table 15.1 Earthquake intensity measures.—cont'd

No.	Earthquake parameter	Definition	Unit	Reference
17	Spectral acceleration at T_1	$S_a(T_1)$	g	Shome et al. (1988)
18	Spectral velocity at T_1	$S_v(T_1)$	m/s	—
19	Spectral displacement at T_1	$S_d(T_1)$	m	—
20	A95 parameter	$A_{95} = 0.764 \cdot I_a^{0.438}$	g	Sarma and Yang (1987)

- $5.0 \leq M_w \leq 7.8$
- $0.07\ \text{Km} \leq R_b \leq 89.76\ \text{Km}$
- $2.79\ \text{s} \leq D_{5\text{-}95} \leq 60.77\ \text{s}$
- $0.04\ \text{s} \leq T_p \leq 1.24\ \text{s}$

The response spectra of ground motions are shown in Fig. 15.6. It should be noted that the mean spectrum of the input motions falls between the spectra of site class A and class B according to Eurocode 8 (EC-8, 2005).

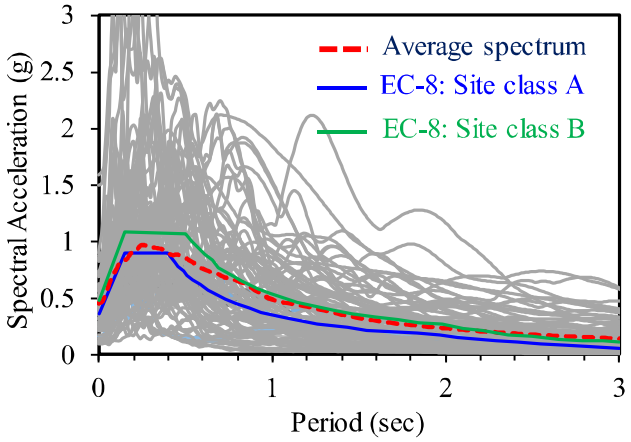

Figure 15.6 Response spectra of ground motions.

5. Probabilistic seismic demand model

A probabilistic seismic demand model (PSDM), which contains the relationship between structural demand and an earthquake IM, needs to be appropriately established in the probabilistic performance-based seismic design (Pejovic et al., 2017). The most common expression of the relationship between seismic demand and earthquake IMs is the power form in Eq. (15.1) (Cornell et al., 2002; Jahangiri et al., 2018; Padgett et al., 2008).

$$S_D = a \times (IM)^b \tag{15.1}$$

where S_D is the median value of structural demand; a and b are the regression coefficients. This equation can be rewritten in forms of linear regression as follows:

$$ln(S_D) = ln(a) + b \times ln(IM) \tag{15.2}$$

The conditional failure probability that the structural demand (D) exceeds its capacity for a given IM in the fragility analysis can be expressed as

$$P_f = P[D \geq d|IM] \tag{15.3}$$

where d is the specified value, normally it is based on the structural capacity. Assuming that the structural demand and capacity follow lognormal distributions, Eq. (15.3) can be rewritten as

$$P[D \geq d|IM] = 1 - \Phi\left[\frac{ln(d) - ln(S_D)}{\sigma_{D|IM}}\right] \tag{15.4}$$

where $\Phi[\text{-}]$ is the standard normal function and $\sigma_{D|IM}$ is the logarithmic standard deviation.

6. Efficiency assessment of bridge response with various IMs

Ground motions are horizontally imposed on the bridge model in the transversal direction (Y-axis). EDP of the bridge is measured in terms of the maximum horizontal displacement of the piers. Then, PSDMs of the bridge are developed for all considered IMs and EDP. The efficiency of IMs is evaluated using statistical indicators of the PSDM, which are the coefficient of determination (R^2), correlation coefficient, and dispersion (i.e., standard deviation). The higher the R^2 and correlation coefficient the more

correlated and efficient IM is. If the standard deviation is lower, the considered IM is more efficient.

Fig. 15.7 shows the scatterings of EDP of the bridge pier P5 in Y-direction with respect to different IMs. It should be noted that the results of all piers are obtained, and a similar trend is observed. Thus, results of a typical pier (i.e., P5) are presented herein for the sake of space. It can be found in Fig. 15.7 that IMs with the largest R^2 of PSDM are $S_a(T_1)$, $S_v(T_1)$, $S_d(T_1)$, ASI, EPA, and PGA. The correlation coefficients and standard deviations of the scatterings for bridge piers with various IMs are shown in Fig. 15.8. It is also observed that the strongest correlated IMs are $S_a(T_1)$, $S_v(T_1)$, $S_d(T_1)$, ASI, EPA, and PGA.

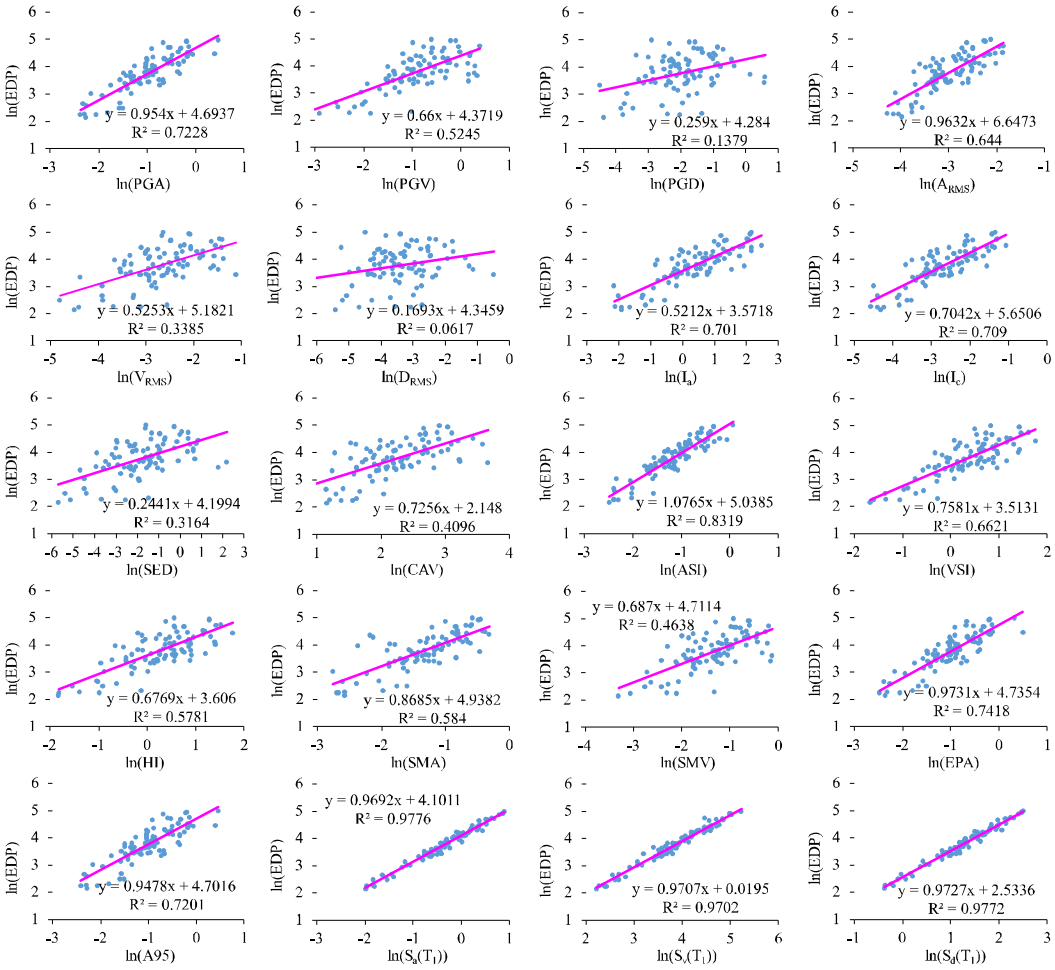

Figure 15.7 Scatterings of EDP with various IMs.

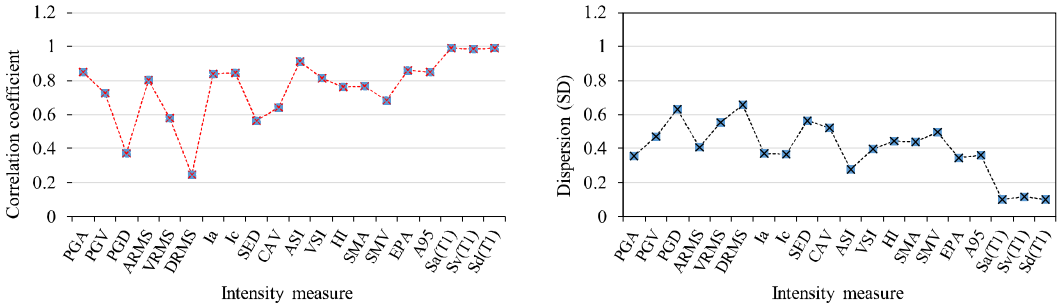

Figure 15.8 Correlation coefficient and dispersions of PSDM of the bridge with various IMs.

7. Concluding remarks

This study develops PDSMs for 20 earthquake IMs and identified the efficient IMs for the seismic performance of a skewed RC bridge. A set of 90 ground motions, which contains a wide range of amplitudes, magnitudes, epicentral distances, significant durations, and predominant periods, is used to perform nonlinear time-history analyses. The numerical analysis results reveal that the efficient IMs for the PDSM of the skewed RC bridge are $S_a(T_1)$, $S_v(T_1)$, $S_d(T_1)$, ASI, EPA, and PGA. Meanwhile, the weakly correlated IMs with the response of skewed bridges are D_{RMS}, PGD, SED, V_{RMS}, and CAV.

References

Abdel-Mohti, A., & Pekcan, G. (2008). Seismic response of skewed RC box-girder bridges. *Earthquake Engineering and Engineering Vibration,* 7(4), 415–426.

Abdel-Mohti, A., & Pekcan, G. (2013). Assessment of seismic performance of skew reinforced concrete box girder bridges. *International Journal of Advanced Structural Engineering, 5*(1), 1–18.

Arias, A. (1970). *Measure of earthquake intensity*. Santiago de Chile: Massachusetts Inst. of Tech., Cambridge. Univ. of Chile.

Avsar, Ö., & Özdemir, G. (2013). Response of seismic-isolated bridges in relation to intensity measures of ordinary and pulselike ground motions. *Journal of Bridge Engineering, 18*(3), 250–260.

Bayat, M., & Daneshjoo, F. (2015). Seismic performance of skewed highway bridges using analytical fragility function methodology. *Computers and Concrete, 16*(5), 723–740.

Benjamin, J. R. (1988). *A criterion for determining exceedance of the operating basis earthquake, Report No.* EPRI NP-5930. Palo Alto, California, USA: Electrical Power Research Institute.

Cao, V., & Ronagh, H. R. (2014). Correlation between seismic parameters of far-fault motions and damage indices of low-rise reinforced concrete frames. *Soil Dynamics and Earthquake Engineering, 66*, 102–112.

Chen, L., & Chen, S. (2016). Seismic fragility performance of skewed and curved bridges in low-to-moderate seismic region. *Earthquakes and Structures, 10*(4), 789–810.

Chen, Z., & Wei, J. (2013). Correlation between ground motion parameters and lining damage indices for mountain tunnels. *Natural Hazards, 65*(3), 1683–1702.

Cornell, C. A., Jalayer, F., Hamburger, R. O., & Foutch, D. A. (2002). Probabilistic basis for 2000 SAC federal emergency management agency steel moment frame guidelines. *Journal of Structural Engineering, 128*(4), 526–533.

CSI. (2015). *SAP2000 - integrated software for structural analysis and design*. Berkeley, CA, USA: Computer and Structures, Inc.

Dobry, R., Idriss, I. M., & Ng, E. (1978). Duration characteristics of horizontal components of strong-motion earthquake records. *Bulletin of the Seismological Society of America, 68*(5), 1487–1520.

EC-8. (2005). *Eurocode 8* - Design of structures for earthquake resistance - Part 1: General rules, seismic actions and rules for buildings. Brussels: European Committee for Standardization.

Elenas, A. (2000). Correlation between seismic acceleration parameters and overall structural damage indices of buildings. *Soil Dynamics and Earthquake Engineering, 20*(1–4), 93–100.

Elenas, A., & Meskouris, K. (2001). Correlation study between seismic acceleration parameters and damage indices of structures. *Engineering Structures, 23*(6), 698–704.

Ghayoomi, M., & Dashti, S. (2015). Effect of ground motion characteristics on seismic soil-foundation-structure interaction. *Earthquake Spectra, 31*(3), 1789–1812.

Housner, G. W. (1952). Spectrum intensities of strong-motion earthquakes. In *Symposium on earthquake and blast effects on structures, (Los Angeles, California, USA)*.

Jahangiri, V., Yazdani, M., & Marefat, M. S. (2018). Intensity measures for the seismic response assessment of plain concrete arch bridges. *Bulletin of Earthquake Engineering, 16*(9), 4225–4248.

Kawashima, K., & Tirasit, P. (2008). Effect of nonlinear seismic torsion on the performance of skewed bridge piers. *Journal of Earthquake Engineering, 12*(6), 980–998.

Kostinakis, K., Athanatopoulou, A., & Morfidis, K. (2015). Correlation between ground motion intensity measures and seismic damage of 3D R/C buildings. *Engineering Structures, 82*, 151–167.

Kramer, S. L. (1996). *Geotechnical earthquake engineering*. Upper Saddle River, New Jersey: Prentice Hall. Inc..

Kun, C., Yang, Z., & Chouw, N. (2018). Seismic performance of skewed bridges with simultaneous effects of pounding and supporting soil. *Engineering Structures, 174*, 26–38.

Lee, T. H., & Nguyen, D. D. (2018). Seismic vulnerability assessment of a continuous steel box girder bridge considering influence of LRB properties. *Sādhanā, 43*(1), 1–15.

Mander, J. B., Priestley, M. J., & Park, R. (1988). Theoretical stress-strain model for confined concrete. *Journal of Structural Engineering, 114*(8), 1804–1826.

Massumi, A., & Gholami, F. (2016). The influence of seismic intensity parameters on structural damage of RC buildings using principal components analysis. *Applied Mathematical Modelling, 40*(3), 2161–2176.

Nguyen, D. D., & Lee, T. H. (2018). Seismic fragility curves of bridge piers accounting for ground motions in Korea. *IOP Conference Series: Earth and Environmental Science, 143*(1), 012029.

Nguyen, D. D., Park, D., Shamsher, S., Nguyen, V. Q., & Lee, T. H. (2019). Seismic vulnerability assessment of rectangular cut-and-cover subway tunnels. *Tunnelling and Underground Space Technology, 86*, 247–261.

Nguyen, D. D., Thusa, B., Han, T. S., & Lee, T. H. (2020). Identifying significant earthquake intensity measures for evaluating seismic damage and fragility of nuclear power plant structures. *Nuclear Engineering and Technology, 52*(1), 192–205.

Nguyen, D. D., Azad, M. S., Choi, B. H., & Lee, T. H. (2020). Efficient earthquake intensity measure for seismic vulnerability of integral abutment bridges. *Journal of the Korean Society of Hazard Mitigation, 20*(6), 251–260.

Nuttli, O. W. (1979). *The relation of sustained maximum ground acceleration and velocity to earthquake intensity and magnitude*. Vicksburg, Mississippi, USA: US Army Engineer Waterways Experiment Station.

Padgett, J. E., Nielson, B. G., & DesRoches, R. (2008). Selection of optimal intensity measures in probabilistic seismic demand models of highway bridge portfolios. *Earthquake Engineering and Structural Dynamics, 37*(5), 711–725.

Park, Y. J., Ang, A. H. S., & Wen, Y. K. (1985). Seismic damage analysis of reinforced concrete buildings. *Journal of Structural Engineering, 111*(4), 740–757.

Park, R., & Paulay, T. (1975). *Reinforced concrete structures*. John Wiley and Sons.

PEER ground motion database. (2019). http://peer.berkeley.edu/peer_ground_motion_database.

Pejovic, J. R., Serdar, N. N., & Pejovic, R. R. (2017). Optimal intensity measures for probabilistic seismic demand models of RC high-rise buildings. *Earthquake and Structures, 13*(3), 221–230.

Phan, H. N., & Paolacci, F. (2016). Efficient intensity measures for probabilistic seismic response analysis of anchored above-ground liquid steel storage tanks. In *Pressure vessels and piping conference*. American Society of Mechanical Engineers.

Qiu, Y., Zhou, C., & Siha, A. (2020). Correlation between earthquake intensity parameters and damage indices of high-rise RC chimneys. *Soil Dynamics and Earthquake Engineering, 137*, 106282.

Sarma, S. K., & Yang, K. S. (1987). An evaluation of strong motion records and a new parameter A95. *Earthquake Engineering and Structural Dynamics, 15*(1), 119–132.

SeismoSignal - a computer program for signal processing of strong-motion data. (2017). Available from: http://www.seismosoft.com.

Shome, N., Cornell, C. A., Bazzurro, P., & Carballo, J. E. (1998). Earthquakes, records, and nonlinear responses. *Earthquake Spectra, 14*(3), 469–500.

Shakib, H., & Jahangiri, V. (2016). Intensity measures for the assessment of the seismic response of buried steel pipelines. *Bulletin of Earthquake Engineering, 14*(4), 1265–1284.

Tran, N. L., Nguyen, T. H., Phan, V. T., & Nguyen, D. D. (2021). Seismic fragility analysis of reinforced concrete piers of steel box girder bridges: A parametric study. *Materials Today: Proceedings, 38*, 2310–2315.

Von Thun, J. L. (1988). *Earthquake ground motions for design and analysis of dams. Earthquake engineering and soil dynamics II-recent advances in ground-motion evaluation*.

Wang, Y., Ibarra, L., & Pantelides, C. (2020). Effect of incidence angle on the seismic performance of skewed bridges retrofitted with buckling-restrained braces. *Engineering Structures, 211*, 110411.

Wei, B., Hu, Z., He, X., & Jiang, L. (2020). Evaluation of optimal ground motion intensity measures and seismic fragility analysis of a multi-pylon cable-stayed bridge with super-high piers in Mountainous Areas. *Soil Dynamics and Earthquake Engineering, 129*, 105945.

Wilson, T., Chen, S., & Mahmoud, H. (2015). Analytical case study on the seismic performance of a curved and skewed reinforced concrete bridge under vertical ground motion. *Engineering Structures, 100*, 128–136.

Wilson, T., Mahmoud, H., & Chen, S. (2014). Seismic performance of skewed and curved reinforced concrete bridges in mountainous states. *Engineering Structures, 70*, 158–167.

Zakeri, B., Padgett, J. E., & Ghodrati Amiri, G. (2015). Fragility assessment for seismically retrofitted skewed reinforced concrete box girder bridges. *Journal of Performance of Constructed Facilities, 29*(2), 04014043.

Zelaschi, C., Monteiro, R., & Pinho, R. (2019). Critical assessment of intensity measures for seismic response of Italian RC bridge portfolios. *Journal of Earthquake Engineering, 23*(6), 980–1000.

Zhang, Y. Y., Ding, Y., & Pang, Y. T. (2015). Selection of optimal intensity measures in seismic damage analysis of cable-stayed bridges subjected to far-fault ground motions. *Journal of Earthquake and Tsunami, 9*(1), 1550003.